scientific reports

Check for updates

OPEN

Tryptic oncopeptide secreted from the gut bacterium *Cronobacter malonaticus* PO3 promotes colorectal cancer

Rajesh Padumane Shastry[1,10]✉, Asif Hameed[1,10]✉, Shukla Banerjee[1], Ashwini Prabhu[2], Sukesh Kumar Bajire[1], Sonnenahalli Rudramurthy Pavan[2], Honagodu Ravichandra Dhanyashree[1], Chinmaya Narayana Kotimoole[1], Paul Stothard[4], Suprith Surya[5], Thottethodi Subrahmanya Keshava Prasad[3]✉, Rohan Shetty[6], Fo-Ting Shen[7,8]✉ & Yashodhar Prabhakar Bhandary[9]

The involvement of *Cronobacter*, which is frequently associated with meningitis and necrotizing enterocolitis, in human colorectal cancer remains unexplored. In this study, we isolate and characterize a novel strain of *C. malonaticus* designated PO3 from a fecal sample of a colon cancer patient and demonstrate its proliferative effects on colorectal cancer both in vitro and in vivo. The secretome of PO3 significantly promoted cell proliferation, as evidenced by increased cell viability, fluorescence intensity, and Ki-67 expression, without inducing cell death. Furthermore, using high-resolution mass spectrometry (HRMS), we identified a novel tryptic oncopeptide designated P506, in the PO3 secretome that promotes colorectal cancer. Synthetic P506 further stimulated human colorectal adenocarcinoma cell line HT-29 cell proliferation in a dose-dependent manner. Experiments with the BALB/c mouse model in vivo revealed that both the PO3 secretome and P506 contributed to the development of colorectal polyps and associated histological changes, including dysplasia and altered colonic architecture. These findings suggest that P506, a potent peptide from the PO3 secretome, may have oncogenic potential, promoting colorectal cancer progression.

Keywords Oncopeptide, Colorectal cancer, Secretome, Necrotizing Enterocolitis, *Enterobacter sakazakii*

Colorectal cancer (CRC) is one of the leading causes of cancer-related morbidity and mortality worldwide[1,2]. The complex etiology of CRC involves a multifactorial interplay between genetic predispositions and environmental influences[3], including lifestyle factors, dietary habits, and gut microbiome[4]. The recent findings particularly on the involvement of the gut microbiome in cancer development highlighted the importance of microbial communities in maintaining gastrointestinal health and influencing systemic diseases, including cancer[5,6]. An imbalance in the gut microbiota, known as dysbiosis, has been associated with a range of pathological conditions, including inflammatory bowel diseases, obesity, diabetes, and various cancers[7,8]. In particular, emerging evidence suggests that dysbiosis may be a significant contributor to CRC, potentially influencing tumor initiation, progression,

[1]Division of Microbiology and Biotechnology, Yenepoya Research Centre, Yenepoya (Deemed to be University), Deralakatte, Mangaluru 575018, India. [2]Division of Cancer Research and Therapeutics, Yenepoya Research Centre, Yenepoya (Deemed to be University), Deralakatte, Mangaluru 575018, India. [3]Center for Systems Biology and Molecular Medicine, Yenepoya Research Centre, Yenepoya (Deemed to be University), Deralakatte, Mangaluru 575018, India. [4]Department of Agricultural, Food and Nutritional Science, University of Alberta, Edmonton, AB T6G 2P5, Canada. [5]Advanced Surgical Skill ENhancement Division (ASSEND), Yenepoya (Deemed to be University), Deralakatte, Mangaluru 575018, India. [6]Department of Surgical Oncology, Yenepoya Medical College Hospital, Yenepoya (Deemed to be University), Deralakatte, Mangaluru 575018, India. [7]Department of Soil and Environmental Sciences, National Chung Hsing University, Taichung 40227, Taiwan. [8]Innovation and Development Center of Sustainable Agriculture (IDCSA), National Chung Hsing University, Taichung 40227, Taiwan. [9]Division of Cell Biology and Molecular Genetics, Yenepoya Research Centre, Yenepoya (Deemed to be University), Deralakatte, Mangaluru 575018, India. [10]Rajesh P. Shastry and Asif Hameed: These authors contributed equally to this work. ✉email: rpshastry@yenepoya.edu.in; asifhameed@yenepoya.edu.in; keshav@yenepoya.edu.in; ftshen@dragon.nchu.edu.tw

and response to treatment[6,9]. Precise identification of oncogenic organisms and their secretary byproducts that underpin cancer onset and progression is essential for proper therapeutic intervention.

Our metagenomics analysis recently showed a significant emergence of rare taxa affiliated with phylum *Bacillota* in the gut of colon cancer patients[1]. Furthermore, there is compelling evidence for broader compositional dissimilarities in the gut microbiome of colorectal cancer patients and strain-specific genomic and proteomic differences in the tumor microenvironment[1,10]. Gut bacteria affiliated with the phylum *Bacillota* such as *Streptococcus gallolyticus*[11,12], *Enterococcus faecalis*[13–15] and *Peptostreptococcus stomatis*[6] have been implicated in colon/colorectal cancer. Similarly, members of the phylum *Bacteroidota*, *Pseudomonadota*, and *Fusobacteriota* such as *Bacteroides fragilis*[16,17], *Escherichia coli*[18], and *Fusobacterium nulceatum*[19–21] have been identified in colon/colorectal cancer.

Strains of the genus *Cronobacter*, earlier known as *Enterobacter sakazakii*[22], were reclassified under the phylum *Pseudomonadata* based on distinguishing molecular features[23]. Members of *Cronobacter* are opportunistic pathogens frequently found in neonatal necrotizing enterocolitis, bacteremia, meningitis, and brain abscess/lesions. *Cronobacter malonaticus* was initially known as *C. sakazakii* subsp. *malonaticus* due to the lack of resolution by 16 S rRNA gene sequencing[24]. The proposal for new species *C. malonaticus*, which accommodated biogroups 5, 9 and 14, was put forth based on distinguishing genotypic and phenotypic characteristics including discreminatory malonate utilization[23]. *C. malonaticus*[23] shares a clinical niche with *C. sakazaki*[25] and can adhere to HT-29 and mouse neuroblastoma cell line N1E-115 [26]. However, its possible involvement in CRC remains unexplored.

Various mechanisms driven by microbes have been implicated in CRC[27]. For example, *F. nucleatum* potentiates intestinal tumorigenesis and modulates the tumor-immune microenvironment[19,20]. The adherence and invasion of *Fusobacterium nucleatum* to colorectal cells and induction of oncogenic and inflammatory responses to stimulate cell proliferation were demonstrated through its unique FadA adhesin. Abed et al. (2012)[21] showed that Fap2 of *F. nucleatum* binds to tumor-expressed Gal-GalNAc and promotes the enrichment of this organism in colorectal adenocarcinoma. While a majority of studies were mainly focused on the direct physical contact between oncogenic bacteria and with host, reports also suggest the involvement of a diffusible toxin from *Bacteroides fragilis* (BFT) to trigger a pro-carcinogenic, multi-step inflammatory cascade requiring IL-17R, NF-kappaB, and Stat3 signaling in colonic epithelial cells[16]. We hypothesized that the discharge of oncogenic molecules by gut bacteria may trigger or exacerbate colon cancer in eukaryotic hosts. We tested this hypothesis by using the secretome of *C. malonaticus* PO3, a bacterial species affiliated to phylum *Pseudomonadata*, isolated from the fecal sample of a cancer patient.

Materials and methods

All methods were carried out in accordance with relevant guidelines and regulations. The animal experiments were reported in accordance with ARRIVE guidelines.

Study population and stool sample collection

All research protocols were executed adhering to stringent ethical guidelines, and prior approval was obtained from the Yenepoya Ethical Committee 1 (Protocol number: YEC-1/2020/050), Mangalore, India. Samples were collected between October 2020 and November 2022 after explicit informed consent from colon cancer participants ($n = 10$) attending the Yenepoya Medical College Hospital, Mangalore. Inclusion criteria were being ≥ 18 years old, and a confirmed diagnosis of colon cancer through colonoscopy, biopsy, and histopathology but devoid of therapeutic intervention. On the other hand, patients who declined informed consent, suffering from recurrent colon cancer, undergoing chemotherapy and/or radiation therapy, and those with a family history of colon cancer were excluded from the study. The stool collection container was provided to the participants after their prior consent and the samples were processed immediately. All standard safety protocols were followed throughout the sample collection and downstream analyses.

Isolation of PO3 from the stool sample

Bacterial strains displaying distinct colony morphology were isolated from freshly collected feces of a colorectal cancer patient after serial dilution with saline peptone water (containing 0.1% peptone and 0.85% NaCl in distilled water) followed by spread-plating onto Brain Heart Infusion (BHI) agar (HiMedia, India). The plates were incubated at 37 °C for 24–48 h and the slow-growing colonies were selected based on the distinguishing morphological features. A pure culture of PO3, which was obtained by multiple streaking on BHI agar followed by plating at Luria Bertani (LB) agar (HiMedia, India), was identified as *Cronobacter* by 16S rRNA gene sequencing, and preserved at -80 °C as 40% (v/v) glycerol stocks.

Preparation of secretome

An overnight culture of PO3 in LB medium was used to inoculate 10 ml of fresh LB medium in a conical flask and incubated at 37 °C with continuous shaking at 120 rpm for 24 h. The cells were harvested by transferring them to a sterile 15 ml tube and centrifuging at 1118 × *g*. The resulting supernatant was passed through a 0.22 µm filter and transferred to a sterile 15 ml tube. The filtered supernatant was subjected to lyophilization to obtain a dried form of the secretome. Various concentrations of secretome (5, 50, and 100 µg/ml) were prepared for subsequent cell viability assays. The cell pellet obtained from centrifugation was resuspended in 1X PBS buffer (HiMedia, India) and subjected to sonication for 5 min at an amplitude of 40% with a 10-second ON/OFF cycle. Following sonication, centrifugation was carried out at 1118 × *g* for 15 min to isolate the secretome. The resulting cell-free lysate and lyophilized cell-free supernatant were stored at 4 °C to preserve until further process.

Assessment of cell-proliferation

MTT assay

To detect the cell proliferation, an MTT assay was performed as per the previously reported method[28]. Briefly, human colorectal adenocarcinoma cell line HT-29 (procured from National Centre for Cell Science (NCCS) in Pune, India) was detached from a T25 flask using trypsin-EDTA (HiMedia, India) and then centrifuged at 600 × *g* for three minutes. The supernatant was discarded, and the cell pellet was resuspended in 1 ml of complete media. The cell count was determined using a hemocytometer, and the cells were subsequently seeded onto a 96-well plate at a density of 5000 cells per well. The plate was then incubated at 37 °C with 5% CO_2 for 24 h to attain confluency. After the 24-hour incubation period, the CFS (5 µg/ml) was added to the cells in the respective wells and incubated for an additional 24 h. Following the incubation, the media in the wells was removed, and 100 µl of MTT reagent (HiMedia, India) at a concentration of 1 mg/ml was added to each well under darkness. The plate was then incubated for 4 h to allow for the formation of formazan crystals by the viable cells. Subsequently, the MTT reagent was carefully removed, and 100 µl of dimethylsulfoxide (DMSO, HiMedia, India) was added to dissolve the MTT crystals. The absorbance of the resulting solution was measured at 570 nm.

Live-dead staining

Cell proliferation of the HT-29 cells was carried out as per the previously reported methods with minor modifications using acridine orange-ethidium bromide (AO-EB, Sigma-Aldrich, India) based fluorescence microscopic analysis[29]. The assay was carried out in 24 well plates seeded with HT-29 (25,000 cells/well), incubated at 37 °C, 5% CO_2 for 24 h. After the incubation period, the cells were treated with 5 µM of P506 (GeNexT Genomics Pvt. Ltd., Nagpur, India) and 100 µg/ml of PO3 supernatant, incubated at 37 °C, 5% CO_2 for 24 h. The cells were washed with PBS and stained with AO-EB (2 µg/ml) for 15 min under dark and observed under the fluorescence microscope using the green and red channels at 20X magnification, compared with the untreated control.

Flow cytometry

Cell cycle analysis of HT-29 cells was performed using flow cytometry after treatment with secretome[29]. The cell suspension was harvested and centrifuged at 120 × *g* for 3 min. The resulting pellet was washed with 10 ml of PBS, centrifuged again, and then resuspended with 0.5 ml of PBS. Subsequently, 4.5 ml of 70% cold ethanol was added dropwise to the suspension with vortexing. The cells were then incubated for 2 h at -20˚C for fixation. After the incubation, the fixed cell suspension was centrifuged at 120 × *g* for 3 min, and the supernatant was discarded. The pellet was washed with 5 ml of FACS buffer and centrifuged. The resulting pellet was resuspended in 100 µl of FACS buffer and 10 µl of Ki-67-FITC antibody (Cell Signalling Technology, India). The suspension was incubated for 30 min under darknes to facilitate specific antibody binding. Following the incubation, the cells were washed again with 5 ml of FACS buffer and centrifuged. To the pellet, 500 µl of PI (Propidium Iodide, Sigma-Aldrich, India) staining solution was added, and the mixture was gently mixed and incubated for 20 min under darknes. PI is used to stain DNA, allowing for the assessment of the cell cycle. Finally, the stained cell suspension was analysed using a flow cytometer with a blue laser (488 nm) and detection filters (530/30 nm bandpass for FITC and 610/20 nm bandpass for PI).

Molecular identification of fecal bacterial isolates

Genus-level identification based on 16 S rRNA gene sequencing

The bacterial genomic DNA was extracted using a previously reported method[30]. To identify the specific bacterial species, the 16 S rRNA gene was amplified using universal forward and reverse primers (27 F, 5′-AGAGTTTGATCCTGGCTCAG-3′ and 1492R, 5′-ACGGCTACCTTGTTACGCTT-3′). The reaction mixture (25 µl) contained 1 µl of primers each, 1 µl of template DNA, and 22 µl of a one-fold diluted master mix (Ampliqon Red Dye Master Mix, Denmark). The amplification was performed with the following thermocycling conditions: an initial denaturation at 94 °C for 5 min, followed by 35 cycles of amplification at 94 °C for 45 s, 54 °C for 45 s, and 72 °C for 1 min. The final step involved polymerization at 94 °C for 8 min. Subsequently, the PCR product was purified and analyzed on a 1.5% agarose gel. The DNA sequencing was carried out, and the resulting sequence was subjected to BLAST analysis.

Species/strain-level identification based on genome sequencing

Genomic DNA was extracted using a commercial DNA extraction kit (Thermo Fisher, USA) according to the manufacturer's instructions and sequenced using Illumina sequencing at Himedia, Mumbai, India. Two-fifty ng of total DNA was used as input for library preparation using QIASeq FX DNA kit (Qiagen) to fragment and obtain adapter-ligated and indexed library as per manufacturer's instructions. The indexed library was sequenced on an Illumina MiSeq using a 300-cycle paired-end chemistry. FASTQC was used to assess the quality of raw fastq files. Quality assessment for genome assemblies generated by Spades[31] and Megahit[32] assemblers was carried out using the Quast[33]. Genome annotation was carried out using Prokka[34]. Phylogenomic analysis was performed using GToTree[35].

The sequence was uploaded to the Rapid Annotations using Subsystems Technology (RAST, http://rast.nmpdr.org/rast.cgi)[36] for automated annotation. BLASTp (https://blast.ncbi.nlm.nih.gov/Blast.cgi) tool was used in addition to confirming gene features of essential biosystems against a non-redundant database of the National Center for Biotechnology Information (NCBI). The genome sequence of PO3 (GCA_047428785.1; BioSample code: SAMN43360089) and other closely related type strains of *Cronobacter* were uploaded to the Type (Strain) Genome Server (https://tygs.dsmz.de/) and compared. Phylogenetic trees were reconstructed for the 16 S rRNA gene and draft genome using TYGS and LPSN[37]. Ortho ANI was used for intergenomic comparison and similarity by average orthologous average nucleotide identity (OrthoANI)[38] by utilizing genomes of type strains

of *Cronobacter* species and nearest strains of *C. malonaticus* retrieved from EzBiocloud. A preliminary circular genome view was obtained from BV-BRC[39]. Comparative genome maps were generated using Proksee[40].

Identification of oncogenic peptide by LC-MS analysis

Sample preparation for LC-MS analysis

The overnight grown cells were centrifuged at 6400 × *g* for 15 min and the supernatant (CFS) was separated. The CFS was lyophilized overnight, and the powdered sample was resuspended (1 mg/ml) in PBS (pH 7.0).

SepPak C18 cartridge-based desalting

The CFS was desalted to remove salts and surfactants present in the samples by Waters SepPak C18 1 cc cartridge. The sample was vacuum evaporated and resuspended with 100 µL of 0.1% formic acid (FA) in water. Desalting was initiated with activation of the C18 bed by passing through 500 µL of 100% acetonitrile, followed by conditioning with 1000 µL of 0.1% FA twice. Later, a sample containing peptides was loaded and passed through the C18 cartridge slowly. Hence, all the peptides were available for the C18 binding. C18 cartridges post-sample loading were washed twice using 0.1% FA to remove unbound contents. Finally, C18 cartridge-bound peptides were eluted slowly by passing 500 µL of 0.1% FA in 40% ACN in water solution twice.

LC-MS/MS by data-dependent acquisition method

Post desalting, the sample was resuspended with 0.1% FA (Mobile Phase A) and acquired in 120 min data-dependent acquisition (DDA) method using EASY-nLC 1200 liquid chromatography system connected to Orbitrap Fusion Tribrid (Thermo Scientific, Bremen, Germany) mass spectrometer. The sample in the well was loaded onto a trap column (Acclaim PepMap™ 100, 75 µm X 2 cm, nanoViper, C18, 3 µm, 100Å) and then made to elute out by passing 0.1% FA in 80% ACN (Mobile Phase B). Whereas, the peptides were separated in the analytical column (PepMap™ RSLC C18, 2 µm, 100Å, 50 µm × 15 cm) by increasing the Mobile Phase B in gradient mode for 120 min with a flow rate of 300 nL/min. The columns equilibrated prior to each run and sample loading was performed by passing mobile phase A (0.1% FA). The percentage of mobile phase B was increased gradually from 5% at 0 min to 35% at 100 min, this was further increased to 60% in 4 min and 100% in another 7 min. Finally, the percentage of mobile phase B was kept at 100% for 9 min. The analytical column temperature was 45 °C throughout the process.

Peptides eluted from the column were ionized in positive ion mode at EASY-Spray™ source with spray voltage and ion transfer tube temperature of 1.9 kV and 275 °C, respectively. Ionized peptides were acquired in DDA mode with 3 sec cycle time. Under Full MS scan, peptide precursors ranging between 400 and 1600 *m/z* were acquired in an Orbitrap mass analyzer with a mass resolution of 120,000. The automatic gain control (AGC) and maximum ion injection time (Max. IT) for the precursor scan were set at $2e^5$ and 50 ms, respectively. Precursors with charge state (*z*) between 1 and 6 and intensity ≥ $5e^3$ were separated using Quadrupole with an isolation window of 1 *m/z*. Quadrupole-isolated precursors were fragmented under HCD with a collision energy of 35 ± 3%. Finally, the fragment ions were acquired in the Orbitrap mass analyzer at 30,000 resolutions. MS/MS scan range mode was set to "Auto" with AGC and Max. IT were $1e^5$ and 200 ms, respectively. All the raw files were searched in the bacterial proteome database using Andromeda search engines in MaxQuant v2.0.1.0.

In vivo tumorigenesis assay

Animal maintenance

Male and female BALB/c mice, aged 6 to 8 weeks (17–20 g), were procured from Spring Labs (Tumakuru, Karnataka, India) and housed in the central laboratory animal facility at Yenepoya (Deemed to be University), Deralakatte, Mangalore, India. All mice were kept in a 12-hour photoperiod under specific pathogen-free conditions, with unrestricted access to water and food throughout the study. The procedures were followed as per the approval from Yenepoya University Institutional Animal Ethics Committee (Approval number: YU/IAEC/P06/2024).

AOM-DSS mouse model

In the AOM-DSS tumorigenesis model, mice were acclimatized for 2 weeks[41]. Each mouse received a single i.p. injection of 10 mg/kg azoxymethane (AOM, Sigma-Aldrich, India) post-acclimatization, followed by the supply of drinking water mixed with 1% dextran sodium sulfate (DSS, HiMedia, India) for a week. Subsequently, we switched their water back to plain water for a week and then reintroduced the 1% DSS. This alternating cycle of DSS and plain water was continued for 8 weeks. At the end of the experiment, the mice were euthanized, and the colon was harvested. The tumors were counted and measured with vernier calipers. Tumor burden was assessed as the total tumor volume per mouse. Colon and associated tumor tissues were either stored at -80 °C or fixed in 10% formalin for further analysis.

PO3 secretome/P506-treated murine tumor model

For the secretome tumorigenesis model, mice were acclimatized for 2 weeks followed by the daily receipt of PO3 secretome (100 µg/kg) through intraperitoneal injections for one week (the dosage was estimated as per previous report[27]). After a week's break, secretome treatment was resumed and this alternate week treatment cycle continued for 8 weeks. The peptide tumorigenesis model followed a similar protocol but with intraperitoneal injection of P506 (125 µM/kg). After 8 weeks, mice were euthanized, and tumor number and volume were measured.

Histopathology

Formalin-fixed colonic tissues were embedded in paraffin and stained with hematoxylin and eosin (H&E, Himedia, India). The slides were examined for abnormal or dysplastic epithelial maturation, characterized by an increased nucleus-to-cytoplasm ratio, and hyperchromatic, enlarged, and irregular nuclei within the crypts.

Immunoblotting

To analyse the expression of Ki67, immunoblotting was performed as per the previously reported method[42]. In brief, HT-29 cells were seeded at a cellular density of 1.5×10^5 onto 10 cm plates and subjected to 48 h of treatment with 10 nM, 1 µM, and 5 µM of P506 as well as and 25, 50,100 µg/ml concentration of crude PO3 secretome. After treatment, the cells were rinsed twice with 1X PBS, lysed using the lysis buffer (2.5 mM sodium pyrophosphate, 4% sodium dodecyl sulfate (SDS), 1 mM sodium orthovanadate, 50 mM triethyl ammonium bicarbonate (TEABC), 1 mM β glycerol phosphate) and sonicating 3 cycles for 2 min each at 30% amplitude using a probe sonicator (Q-Sonica, Cole-Parmer, India). A dry bath was used to incubate the lysate for 10 min at 95 °C and centrifuged at 6400 × *g* for 20 min. The total protein concentration was estimated using the BCA kit method.

Using immunoblotting, the expression of Ki67 and β-actin was investigated. Initially, the same quantity of protein from each group was loaded onto SDS PAGE, resolved at 80 V for 15 min, and then increased to 120 V. Following protein separation, proteins were transferred to nitrocellulose membranes for 2 h at 250 mA for β-actin and 1 h at 500 mA for Ki67 at 4 °C. The membrane was blocked using skimmed milk, and subsequently incubated separately for the respective blots overnight at 4 °C with primary Ki67 and conjugated β-actin antibody. After 2 h of room temperature incubation with the Ki67 secondary antibody, the Ki67 and β-actin blots were washed three times with 1X PBST, visualized with ECL substrate, and the expression was recorded using the gel documentation system. The protein expression of different groups was analysed through ImageJ.

Statistical analysis

Statistical significances ($*p < 0.05$, $**p < 0.01$, $***p < 0.001$) for culture-based assays were estimated through One-way ANOVA and/or *t*-test (specified in the image) using GraphPad Prism.

Results

C. malonaticus PO3 genome analysis

PO3 genome was sequenced to gain insights into its phylogenomics, genetic makeup and metabolic capabilities. A 4.6 Mb genome (53 contigs) harboured 56.8 mol% G + C, 4474 coding sequences, and 77 rRNA. The 16 S rRNA gene- and genome-based phylogeny revealed unique and strong (90–100% bootstrap support) taxonomic lineages (Fig. S1a–b) attained by PO3 within the clade that accommodated *C. sakazaki* NBRC 102416^T and *C. malonaticus* LMG 23826^T (Fig. S2a–b). The tight phyletic association found between PO3 and *C. malonaticus* LMG 23826^T (90% confidence of the node (Fig. S1b) and the highest OrthoANI (99.8%) and dDDH (95%) values obtained during genomic analysis confirmed PO3 as a new strain of *C. malonaticus*. Furthermore, the isolate PO3 is listed in the PubMLST database[43] as *C. malonaticus* sequence type 7, a common sequence type found in adult infections.

C. malonaticus PO3 secretome promotes human colorectal adenocarcinoma

At first, PO3 secretome was tested on the metabolism and proliferation of human colorectal adenocarcinoma cell line HT-29. Cell viability assay (performed after 24 h of incubation) revealed a significant ($p < 0.01$) increase in MTT dye reduction in HT-29 cells when treated with PO3 secretome at a dose of 100 µg/ml (Fig. 1a). No signs of cell death were recorded at the tested dose. In contrast, a significant ($p < 0.01$) increase in the fluorescence intensity suggested the possible proliferation of PO3-treated HT-29 cells (Fig. 1b–c). Flow cytometry analysis displayed an increased ($p = 0.0597$) signal in PO3-treated HT-29 cells corresponding to the proliferative marker Ki-67 (Fig. 1d–f). Furthermore, the expression of Ki-67 upon treatment with PO3 revealed the promotion of cell proliferation (Fig. 1g–h). These data indicated that the PO3 secretome promotes HT-29 cell division.

Identification of P506 as a potential tryptic oncopeptide secreted by *C. malonaticus* PO3

The secretome of PO3 was subjected to high resolution mass spectrometry (HR-MS) for peptidome profiling. We found 251 peptides in the secretome of PO3 that were further filtered based on their quorum sensing features and capability of penetrating BBB. Among short-listed peptides, P506 (RHLEFFNT, mol wt: 1.06 kDa; *m/z*: 1063.50 $[M+H]^+$) met the basic dual-criterion of being putative quorum sensing (filtered through QSPpred[44]) and breaching BBB attributes (Predicted by BBPpred[45]) (Fig. 1i–k). We identified a mannose-specific phosphotransferase system (PTS) that could serve as a precursor for P506 (Fig. S2a–b) in PO3. P506 can be formed by digesting mannose-PTS with trypsin, a gastric enzyme. P506 (RFLEFFNT) constituted a terminal threonine residue when associated with mannose PTS, possibly susceptible to kinase activity governed by cyclin-dependent protein kinase Cdk1/Cdc2. We procured high purity (> 96.7%) synthetic P506 in acetate salt form (GeNexT Genomics Pvt. Ltd., Nagpur, India) and assessed its impacts on the metabolism and proliferation of HT-29 cells.

Synthetic P506 promotes human colorectal adenocarcinoma cell line HT-29

We found a significantly increased MTT signal for HT-29 with increasing doses of synthetic P506 (1–5 µM) suggesting high metabolic activity (Fig. 2a). Live-dead cell assay confirmed the proliferation of HT-29 (5 µM P506) (Fig. 2b–c), which was further corroborated by increased ($p < 0.01$) fluorescence intensity while no signs of cell death were recorded (Fig. 2f–g). Dose-dependent impact of P506 on HT-29 cells was evident through Ki-67 based western blot analysis (Fig. 2d–e). These results indicated the proliferative attributes of P506 on HT-29 cells.

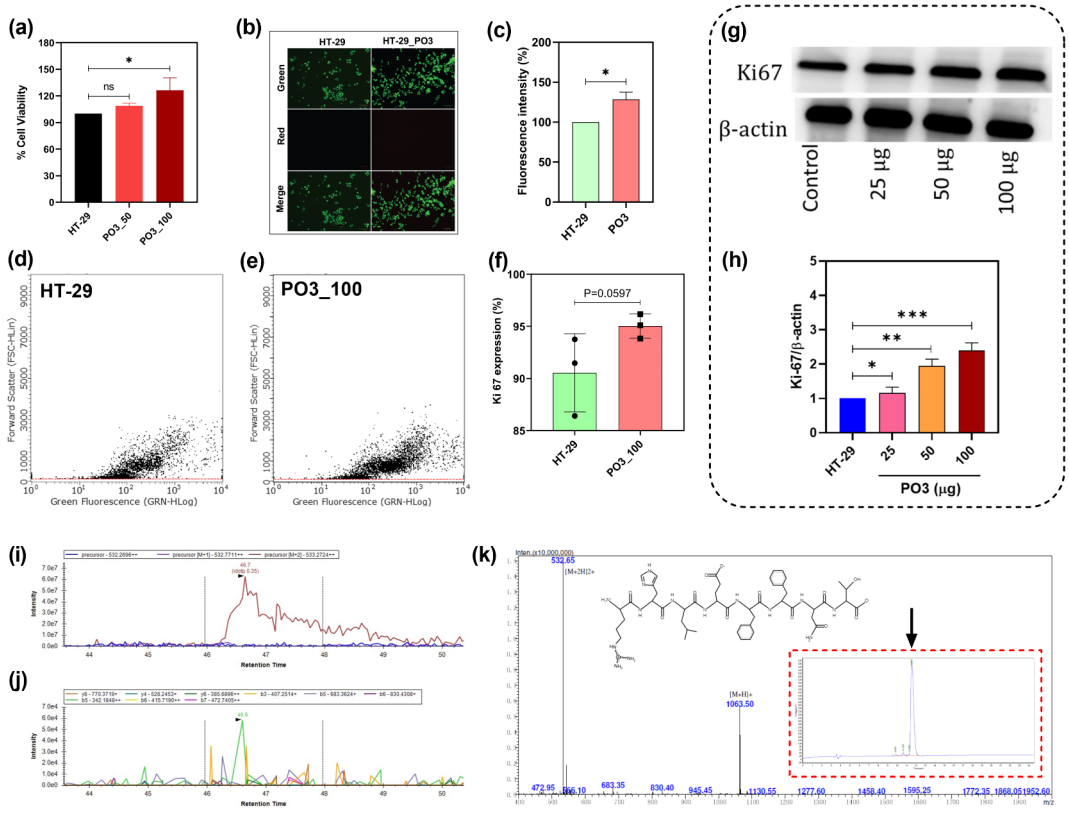

Fig. 1. Proliferative activity of *Cronobacter malonaticus* PO3 secretome on human colorectal adenocarcinoma cell line HT-29 and identification of an oncopeptide P506 (RHLEFFNT). Results of cell viability assay based on MTT (**a**), live-dead cell assay (**b**), Ki-67 expression as determined by FACS (**c**–**e**), Ki-67 expression as determined by western blot (**g**–**h**) are shown. Statistical significance was calculated by t test. $^{*}p < 0.05$, $^{**}p < 0.01$, $^{***}p < 0.001$. Data points are mean ± SD ($n = 3$). MS/MS spectra showing the retention time and molecular mass of precursors and fragments of oncopeptide P506 (**i**–**j**). *m/z* values of parent ion and collision-induced dissociation fragments of synthetic P506 (**k**); inset, chromatogram showing the P506 peak (arrow head).

PO3 secretome and P506 exhibit tumorigenicity in murine model

We investigated the effects of PO3 secretome and P506 in two different experimental approaches on colorectal cancer development in a BALB/c mouse model (Fig. 3a–d). In the first method, PO3 secretome was administered intraperitoneally daily for 8 weeks to a group of mice ($n = 6$). This approach was aimed to investigate whether secretome could trigger CRC. Interestingly, results showed the development of colorectal polyps, which was evident through histological changes. In the second method, synthetic P506 was administered intraperitoneally every 7th day over 8 weeks. A significant increase in the count and burden of the tumor was recorded in the animals treated particularly with P506 followed by PO3 secretome and AOM (Fig. 3e–f). Dysplastic colonic epithelium along with the increased nuclear to cytoplasmic ratio, increase in the number of colonic crypts, infiltration of neutrophils and a typical cribriform architecture was observed in the samples derived from AOM, PO3 secretome and P506 treatments (Fig. 3g). Colonic sections from the untreated control mice displayed the typical histological features of the normal colonic epithelium with the presence of crypts and normochromic nuclei. Sections from the positive control group, AZM-DSS treated mice showed the presence of hyperchromatic pencillate nuclei with the increased number of crypts and increased nuclei-cytoplasmic ratio. Taken together, P506 is one of the potent oncogenic peptides present in PO3 secretome that triggered the development of colon polyps and associated histopathological changes in the colorectal tissues.

Discussion

The precise identification of *Cronobacter* at the species level was necessary to understand its role in pathophysiology; however, the identification was challenging due to the poor taxonomic resolution offered by traditional 16 S rRNA gene sequence-based analysis. On the other hand, multilocus sequence typing (MLST), one of the DNA-based molecular tools, has been used widely to discriminate *Cronobacter* species and/or pathovars[46–51]. MLST adopts partial sequence analysis of concatenated seven housekeeping genes: *atpD*, *fusA*, *glnS*, *gltB*, *gyrB*, *infB*, and *ppsA*[48]. The concatenated sequences (3,036 bp) can be assigned as a novel sequence type (ST) based on the nucleotide polymorphism that can be traced through *Cronobacter* PubMLST reference database (http://pubmlst.org/cronobacter). The MLST tool has aided the recognition of *C. sakazakii* CC4 associated with neonatal

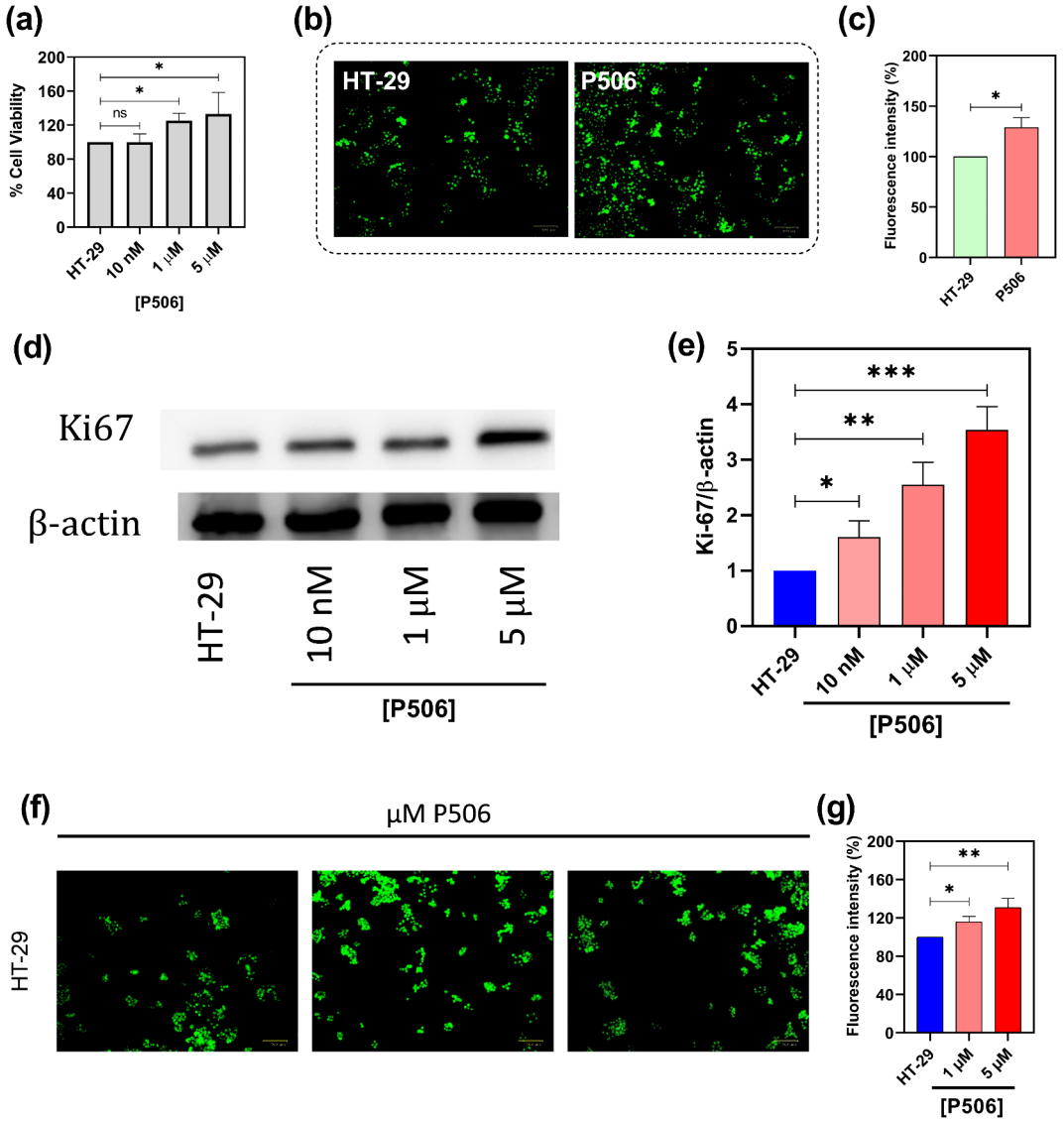

Fig. 2. Proliferative activity of synthetic P506 on human colorectal adenocarcinoma cell line HT-29. Results of cell viability assay based on MTT (**a**) and live-dead cell assay (**b**–**c**) confirming the proliferative impacts of P506 on HT-29. Dose-dependent response of P506 on Ki67 expression in HT-29 (**d**–**e**). Live-dead cell assay confirming dose-dependent impact of P506 on the proliferation of HT-29 cells (**f**–**g**). Statistical significance was calculated by t test. $^{*}p < 0.05$, $^{**}p < 0.01$, $^{***}p < 0.001$, ns, non-significant. Data points are mean ± SD ($n = 3$).

meningitis, *C. sakazakii* ST12 associated with necrotizing enterocolitis, and *C. malonaticus* CC7 with adult infections[46,49–51]. In addition, MLST has been used to reclassify *C. universalis* and *C. condimenti*[50]. Sequence (type ST 7) obtained through PubMLST database reflected the possible ability of PO3 to infect adults.

In contrast, the advent of whole genome sequencing and cutting-edge analytical bioinformatics tools have guided the rapid and precise identification of bacterial pathogens and their metabolic pathways associated with humans and other eukaryotes. Genome sequencing not only assisted the identification of PO3 as a novel strain of *C. malonaticus*, but also helped to trace possible precursor protein that yields oncopeptide P506. Quorum sensing peptides such as PhrG (from *Bacillus subtilis*) and CSP (*Streptococcus mitis*) are implicated in angiogenesis and invasion of breast cancer cells[52] and EDF (from *E. coli*) showed HCT-8/E11 colon cancer cell invasion[53]. Peptides deserve more attention in development as epigenetic modulators, and there is a significant knowledge gap that persists[54]. An earlier study showed that the lipopolysaccharides of *C. malonaticus* exacerbate intestinal infection in mice by altering gut microbe profile, tight junction protein expression, and releasing inflammatory factors in a time- and dose-dependent manner[55]. However, information on the peptides discharged from *C. malonaticus* that could potentially trigger colorectal cancer remains elusive. Given the fecal origin of *C. malonaticus* PO3 from a colon cancer patient, it was hypothesized that this bacterium's secretome could have an oncogenic potential. Indeed, in vitro assays on the human colorectal adenocarcinoma cell line HT-29 revealed a significant increase in cell viability, as indicated by MTT assays, following treatment with the PO3 secretome. Our results also demonstrated an increase in fluorescence intensity and Ki-67 expression, a marker of cell proliferation, following

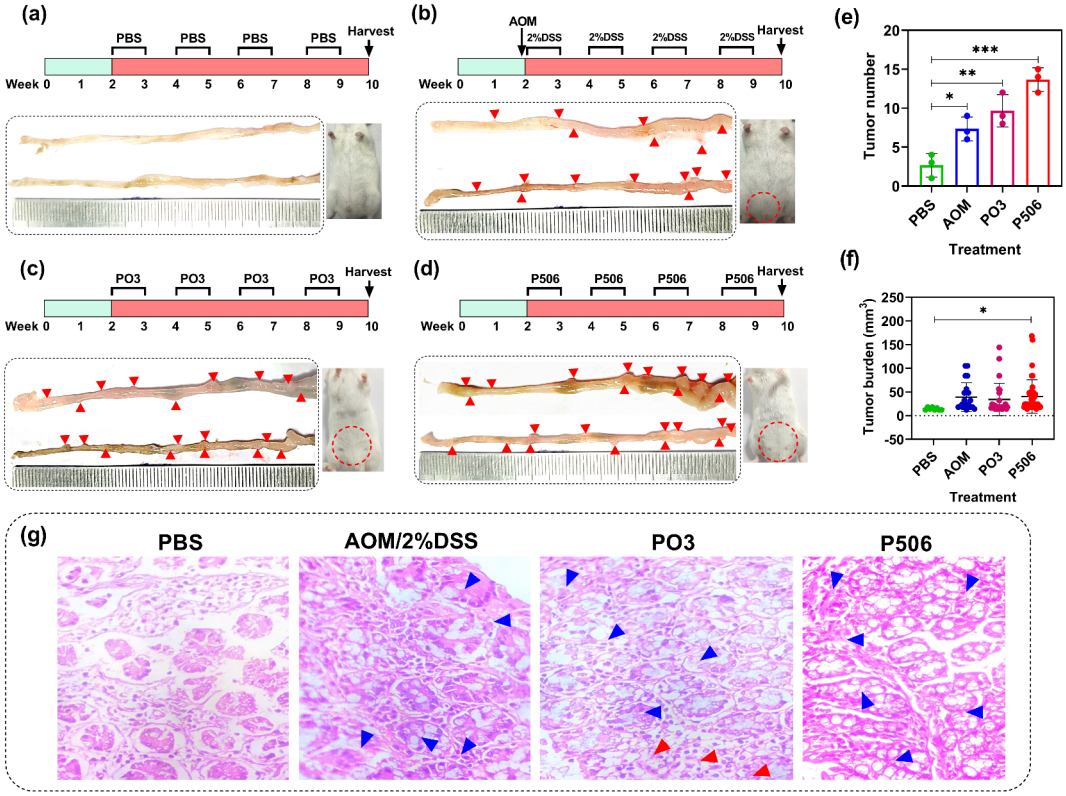

Fig. 3. In vivo validation of the tumorigenicity of the secretome of *Cronobacter malonaticus* PO3 and synthetic P506 using BALB/c mouse model. Treatment time line and the morphology of colons of animals treated with PBS ($n = 3$) (**a**), azoxymethane (10 mg/kg) followed by 2% DSS (**b**), PO3 secretome (100 µg/kg) (**c**), and P506 (125 µM/kg) (**d**) are shown. Corresponding tumor number (**e**) and tumor burden (**f**) are shown in bar charts. (**g**) Histopathology analysis, PBS: Normal histology showing crypts and normochromic nuclei, AOM/2%DSS: Crypt multiplicity with increased nuclei-cytoplasm ratio, hyperchromatic pencillate nuclei, PO3: Blue arrows indicate increased colonic crypts with hyperchromatic nuclei, increased nuclei-cytoplasm ratio; red arrows indicate infiltration of neutrophils, P506: Cribiform architecture with dysplastic epithelium. Statistical significance (in **e** and **f**) was calculated by t test. $^{*}p < 0.05$, $^{**}p < 0.01$, $^{***}p < 0.001$.

PO3 secretome treatment, indicating a direct stimulatory effect on HT-29 cell division. Notably, no significant cell death was observed, emphasizing that PO3 secretome may not induce cytotoxicity but rather supports cancer cell growth, reinforcing the hypothesis that *C. malonaticus* PO3 could contribute to CRC development.

Using high-resolution mass spectrometry (HR-MS), we identified 251 peptides in the PO3 secretome. After filtering for quorum-sensing attributes P506 was selected for further investigation. This peptide's ability to promote CRC cell proliferation was evaluated by synthesizing P506 and testing its effects on HT-29 cells. These results are consistent with studies demonstrating that bacterial-derived peptides can influence host cell behavior and potentially drive oncogenesis. *Clostridium difficile* toxins have been shown to alter epithelial cell growth and contribute to colorectal disease[56]. The impact of P506 on HT-29 cells highlights the potential of bacterial peptides to act as oncogenic factors in the gut microbiome[27].

The in vivo effects of PO3 secretome and synthetic P506 were investigated in a BALB/c mouse model, providing a more comprehensive understanding of their role in tumor development. Mice administered with PO3 secretome or synthetic P506 intraperitoneally over 8-week period showed significant tumorigenesis, as evidenced by the development of colorectal polyps and histopathological changes, including dysplastic epithelium, an increase in colonic crypts, and altered nuclear morphology. These observations are consistent with previous studies where bacterial components or secretomes have been linked to tumor formation in animal models[5,57,58]. For instance, studies have shown that the enteric pathogen *Enterococcus faecalis* can promote colorectal tumorigenesis by releasing extracellular proteins that modify the host immune response and induce epithelial cell proliferation[59–61]. The histopathological changes observed in our study following PO3 secretome or P506 treatment further corroborate the idea that bacterial factors, particularly P506, could contribute to CRC development in vivo. Ultra-high performance liquid chromatography tandem quadrupole mass spectrometry (RP-UPLC-TQ-MS) of serum sample detected EntF* (>100 pM), a quorum sensing peptide that promoted colorectal cancer metastasis in mice[27]. However, further studies using RP-UPLC-TQ-MS are needed to detect qualitatively and quantitatively P506 in the body fluids of mice. The molecular mechanisms underlying the oncogenic effects of P506 remain to be fully elucidated. However, our data suggest that P506 may act through pathways that regulate cell cycle progression and proliferation, as indicated by the increased Ki-67 expression.

Additionally, the interaction of P506 with host signaling pathways may play a crucial role in its oncogenic activity. Further studies focusing on the specific cellular pathways activated by P506, such as cyclin-dependent kinase (CDK) signaling, are necessary to better understand its mode of action and its potential as a therapeutic target.

Conclusion

This study identified the potential ability of the gut bacterium *Cronobacter malonaticus* PO3 to secrete oncopeptide P506 that could trigger onset and development of CRC in vivo and in vitro. The identification of P506 as a potent oncogenic peptide, capable of enhancing cell proliferation and tumorigenesis, underscores the importance of microbial-derived factors in cancer pathogenesis. The conditions that aid P506 to breach the colonic mucin layer and facilitate its penetration into gut epithelial cells warrant further investigations.

Data availability

The whole genomic data is available in the NCBI BioProject PRJNA1153398.

Received: 24 January 2025; Accepted: 17 March 2025
Published online: 22 March 2025

References

1. Shastry, R. P. et al. Emergence of rare and low abundant anaerobic gut firmicutes is associated with a significant downfall of *Klebsiella* in human colon cancer. *Microb. Pathog.* **193**, 106726 (2024).
2. O'Keefe, S. J. D. Diet, microorganisms and their metabolites, and colon cancer. *Nat. Rev. Gastroenterol. Hepatol.* **13**, 691–706 (2016).
3. Catania, F. et al. Global climate change, diet, and the complex relationship between human host and microbiome: towards an integrated picture. *BioEssays* **43**, 2100049 (2021).
4. Qin, Y. et al. Combined effects of host genetics and diet on human gut microbiota and incident disease in a single population cohort. *Nat. Genet.* **54**, 134–142 (2022).
5. Zepeda-Rivera, M. et al. A distinct *Fusobacterium nucleatum* clade dominates the colorectal cancer niche. *Nature* **628**, 424–432 (2024).
6. Tang, Q. et al. Endogenous coriobacteriaceae enriched by a high-fat diet promotes colorectal tumorigenesis through the CPT1A-ERK axis. *Npj Biofilms Microbiomes*. **10**, 1–15 (2024).
7. Pal, P. & Shastry, R. P. Exploring the complex role of gut microbiome in the development of precision medicine strategies for targeting microbial imbalance-induced colon cancer. *Folia Microbiol. (Praha)*. **68**, 691–701 (2023).
8. Shastry, R. P. & Rekha, P. D. Bacterial cross talk with gut microbiome and its implications: a short review. *Folia Microbiol. (Praha)*. **66**, 15–24 (2021).
9. DeGruttola, A. K., Low, D., Mizoguchi, A. & Mizoguchi, E. Current understanding of dysbiosis in disease in human and animal models. *Inflamm. Bowel Dis.* **22**, 1137–1150 (2016).
10. Kordahi, M. C. et al. Genomic and functional characterization of a mucosal symbiont involved in early-stage colorectal cancer. *Cell. Host Microbe*. **29**, 1589–1598e6 (2021).
11. Boleij, A. et al. Novel clues on the specific association of *Streptococcus gallolyticus* subsp. *gallolyticus* with colorectal cancer. *J. Infect. Dis.* **203**, 1101–1109 (2011).
12. Boleij, A. & Tjalsma, H. The itinerary of *Streptococcus gallolyticus* infection in patients with colonic malignant disease. *Lancet Infect. Dis.* **13**, 719–724 (2013).
13. Wang, X. et al. *Enterococcus faecalis* induces aneuploidy and tetraploidy in colonic epithelial cells through a bystander effect. *Cancer Res.* **68**, 9909–9917 (2008).
14. Wang, X. et al. 4-hydroxy-2-nonenal mediates genotoxicity and bystander effects caused by *Enterococcus faecalis*-infected macrophages. *Gastroenterology* **142**, 543–551e7 (2012).
15. Yang, Y. et al. Colon macrophages polarized by commensal bacteria cause colitis and cancer through the bystander effect. *Translational Oncol.* **6**, 596–IN8 (2013).
16. Chung, L. et al. *Bacteroides fragilis* toxin coordinates a pro-carcinogenic inflammatory cascade via targeting of colonic epithelial cells. *Cell. Host Microbe*. **23**, 203–214e5 (2018).
17. Sears, C. L. Enterotoxigenic *Bacteroides fragilis*: a rogue among symbiotes. *Clin. Microbiol. Rev.* **22**, 349–369 (2009). Table of Contents.
18. Sears, C. L. & Garrett, W. S. Microbes, microbiota and colon cancer. *Cell. Host Microbe*. **15**, 317–328 (2014).
19. Kostic, A. D. et al. *Fusobacterium nucleatum* potentiates intestinal tumorigenesis and modulates the tumor-immune microenvironment. *Cell. Host Microbe*. **14**, 207–215 (2013).
20. Rubinstein, M. R. et al. *Fusobacterium nucleatum* promotes colorectal carcinogenesis by modulating E-cadherin/β-catenin signaling via its FadA adhesin. *Cell. Host Microbe*. **14**, 195–206 (2013).
21. Abed, J. et al. Fap2 mediates *Fusobacterium nucleatum* colorectal adenocarcinoma enrichment by binding to Tumor-Expressed Gal-GalNAc. *Cell. Host Microbe*. **20**, 215–225 (2016).
22. Farmer, J. J., Asbury, M. A., Hickman, F. W., Brenner, D. J. & The *Enterobacteriaceae* Study Group. *Enterobacter sakazakii*: A new species of "*Enterobacteriaceae*" isolated from clinical specimens. *Int. J. Syst. Evol. MicroBiol.* **30**, 569–584 (1980).
23. Iversen, C. et al. *Cronobacter* gen. nov., a new genus to accommodate the biogroups of *Enterobacter Sakazakii*, and proposal of *Cronobacter sakazakii* gen. nov., comb. nov., *Cronobacter malonaticus* sp. nov., *Cronobacter turicensis* sp. nov., *Cronobacter muytjensii* sp. nov., *Cronobacter dublinensis* sp. nov., *Cronobacter* genomospecies 1, and of three subspecies, *Cronobacter dublinensis* subsp. *dublinensis* subsp. nov., *Cronobacter dublinensis* subsp. *lausannensis* subsp. nov. and *Cronobacter dublinensis* subsp. *lactaridi* subsp. nov. *Int. J. Syst. Evol. Microbiol.* **58**, 1442–1447 (2008).
24. Iversen, C. et al. The taxonomy of *Enterobacter sakazakii*: proposal of a new genus *Cronobacter* gen. nov. and descriptions of *Cronobacter sakazakii* comb. nov. *Cronobacter sakazakii* subsp. *sakazakii*, comb. nov., *Cronobacter sakazakii* subsp. *malonaticus* subsp. nov., *Cronobacter turicensis* sp. nov., *Cronobacter muytjensii* sp. nov., *Cronobacter dublinensis* sp. nov. and *Cronobacter* genomospecies 1. *BMC Evol. Biol.* **7**, 64 (2007).
25. Li, X. et al. Duplex Real-Time PCR method for the differentiation of *Cronobacter sakazakii* and *Cronobacter malonaticus*. *J. Food. Prot.* **80**, 50–56 (2017).
26. Holý, O. et al. Occurrence of virulence factors in *Cronobacter sakazakii* and *Cronobacter malonaticus* originated from clinical samples. *Microb. Pathog.* **127**, 250–256 (2019).
27. Wynendaele, E. et al. The quorum sensing peptide EntF* promotes colorectal cancer metastasis in mice: a new factor in the host-microbiome interaction. *BMC Biol.* **20**, 151 (2022).
28. Rai, Y. et al. Mitochondrial biogenesis and metabolic hyperactivation limits the application of MTT assay in the estimation of radiation induced growth inhibition. *Sci. Rep.* **8**, 1531 (2018).

29. Lay, M. M., Karsani, S. A. & Abd Malek, S. N. Induction of Apoptosis of 2,4′,6-Trihydroxybenzophenone in HT-29 Colon Carcinoma Cell Line. BioMed Research International 468157 (2014). (2014).
30. Bajire, S. K., Prabhu, A., Bhandary, Y. P., Irfan, K. M. & Shastry, R. P. 7-Ethoxycoumarin rescued *Caenorhabditis elegans* from infection of COPD derived clinical isolate *Pseudomonas aeruginosa* through virulence and biofilm Inhibition via targeting Rhl and Pqs quorum sensing systems. *World J. Microbiol. Biotechnol.* **39**, 208 (2023).
31. Bankevich, A. et al. SPAdes: a new genome assembly algorithm and its applications to single-cell sequencing. *J. Comput. Biol.* **19**, 455–477 (2012).
32. Li, D., Liu, C. M., Luo, R., Sadakane, K. & Lam, T. W. MEGAHIT: an ultra-fast single-node solution for large and complex metagenomics assembly via succinct de Bruijn graph. *Bioinformatics* **31**, 1674–1676 (2015).
33. Gurevich, A., Saveliev, V., Vyahhi, N. & Tesler, G. QUAST: quality assessment tool for genome assemblies. *Bioinformatics* **29**, 1072–1075 (2013).
34. Seemann, T. Prokka: rapid prokaryotic genome annotation. *Bioinformatics* **30**, 2068–2069 (2014).
35. Lee, M. D. GToTree: a user-friendly workflow for phylogenomics. *Bioinformatics* **35**, 4162–4164 (2019).
36. Aziz, R. K. et al. The RAST server: rapid annotations using subsystems technology. *BMC Genom.* **9**, 75 (2008).
37. Meier-Kolthoff, J. P., Carbasse, J. S., Peinado-Olarte, R. L. & Göker, M. TYGS and LPSN: a database tandem for fast and reliable genome-based classification and nomenclature of prokaryotes. *Nucleic Acids Res.* **50**, D801–D807 (2022).
38. Lee, I., Kim, O., Park, Y., Chun, J. & S.-C. & OrthoANI: an improved algorithm and software for calculating average nucleotide identity. *Int. J. Syst. Evol. Microbiol.* **66**, 1100–1103 (2016).
39. Olson, R. D. et al. Introducing the bacterial and viral bioinformatics resource center (BV-BRC): a resource combining PATRIC, IRD and vipr. *Nucleic Acids Res.* **51**, D678–D689 (2023).
40. Grant, J. R. et al. Proksee: in-depth characterization and visualization of bacterial genomes. *Nucleic Acids Res.* **51**, W484–W492 (2023).
41. Huang, P. et al. *Peptostreptococcus stomatis* promotes colonic tumorigenesis and receptor tyrosine kinase inhibitor resistance by activating ERBB2-MAPK. *Cell. Host Microbe.* **32**, 1365–1379e10 (2024).
42. Miller, I. et al. Ki67 is a graded rather than a binary marker of proliferation versus quiescence. *Cell. Rep.* **24**, 1105–1112e5 (2018).
43. Jolley, K. A., Bray, J. E. & Maiden, M. C. J. Open-access bacterial population genomics: BIGSdb software, the PubMLST.org website and their applications. *Wellcome Open. Res.* **3**, 124 (2018).
44. Rajput, A., Gupta, A. K. & Kumar, M. Prediction and analysis of quorum sensing peptides based on sequence features. *PLoS One.* **10**, e0120066 (2015).
45. Dai, R. et al. BBPpred: Sequence-Based Prediction of Blood-Brain Barrier Peptides with Feature Representation Learning and Logistic Regression. *J. Chem. Inf. Model.* **61**, 525–534 (2021).
46. Forsythe, S. J., Dickins, B. & Jolley, K. A. *Cronobacter*, the emergent bacterial pathogen *Enterobacter sakazakii* comes of age; MLST and whole genome sequence analysis. *BMC Genom.* **15**, 1121 (2014).
47. Forsythe, S. J. Updates on the *Cronobacter* genus. *Annu. Rev. Food Sci. Technol.* **9**, 23–44 (2018).
48. Baldwin, A. et al. Multilocus sequence typing of *Cronobacter sakazakii* and *Cronobacter malonaticus* reveals stable clonal structures with clinical significance which do not correlate with biotypes. *BMC Microbiol.* **9**, 223 (2009).
49. Hariri, S., Joseph, S. & Forsythe, S. J. *Cronobacter Sakazakii* ST4 strains and neonatal meningitis, united States. *Emerg. Infect. Dis.* **19**, 175–177 (2013).
50. Joseph, S. et al. *Cronobacter condimenti* sp. nov., isolated from spiced meat, and *Cronobacter universalis* sp. nov., a species designation for *Cronobacter* sp. genomospecies 1, recovered from a leg infection, water and food ingredients. *Int. J. Syst. Evol. Microbiol.* **62**, 1277–1283 (2012).
51. Joseph, S. & Forsythe, S. Insights into the emergent bacterial pathogen *Cronobacter* spp., generated by multilocus sequence typing and analysis. *Front. Microbiol.* **3**, 1-11 (2012).
52. De Spiegeleer, B. et al. The quorum sensing peptides PhrG, CSP and EDF promote angiogenesis and invasion of breast cancer cells *in vitro*. *PLoS ONE.* **10**, e0119471 (2015).
53. Wynendaele, E. et al. Crosstalk between the microbiome and cancer cells by quorum sensing peptides. *Peptides* **64**, 40–48 (2015).
54. Janssens, Y., Wynendaele, E., Vanden Berghe, W. & De Spiegeleer, B. Peptides as epigenetic modulators: therapeutic implications. *Clin. Epigenetics*. **11**, 101 (2019).
55. Ling, N. et al. *Bacteroides fragilis* ameliorates *Cronobacter malonaticus* lipopolysaccharide-induced pathological injury through modulation of the intestinal microbiota. *Front. Immunol.* **13**, 931871 (2022).
56. Chandrasekaran, R. & Lacy, D. B. The role of toxins in *Clostridium difficile* infection. *FEMS Microbiol. Rev.* **41**, 723–750 (2017).
57. Taddese, R. et al. Growth rate alterations of human colorectal cancer cells by 157 gut bacteria. *Gut Microbes*. **12**, 1799733 (2020).
58. Zhang, S. et al. Tumor initiation and early tumorigenesis: molecular mechanisms and interventional targets. *Sig Transduct. Target. Ther.* **9**, 1–36 (2024).
59. Boonanantanasarn, K. et al. *Enterococcus faecalis* enhances cell proliferation through hydrogen peroxide-Mediated epidermal growth factor receptor activation. *Infect. Immun.* **80**, 3545–3558 (2012).
60. Zhang, L. et al. The pathogenicity of vancomycin-resistant *Enterococcus faecalis* to colon cancer cells. *BMC Infect. Dis.* **24**, 230 (2024).
61. Archambaud, C., Nunez, N., da Silva, R. A. G., Kline, K. A. & Serror, P. *Enterococcus faecalis*: an overlooked cell invader. *Microbiol. Mol. Biol. Rev.* **88**, e00069–e00024 (2024).

Acknowledgements

This study was supported by ICMR-DHR, Government of India, New Delhi (ICMR/5/13/84/2020/NCD-III dated 16/03/2021).

Author contributions

R.P.S: Conceptualization, methodology, writing – original draft, funding acquisition, supervision, resources, data analysis. A.H: Conceptualization, methodology, writing – original draft, supervision, resources, data analysis. S.B: Investigation, data analysis. A.P: Investigation, writing – review & editing. S.K.B: Investigation. P.S.R: Investigation. D.H.R: Investigation. C.N.K: Investigation. P.S: Writing – review & editing, data analysis. S.S: Investigation, writing – review & editing. T.S.K.P: Writing – review & editing, resources, methodology. R.S: Writing – review & editing, supervision. F.T.S: – review & editing, resources, data analysis. Y.P.B: Writing – review & editing, supervision, funding acquisition.

Declarations

Competing interests

The authors declare no competing interests.

Ethical approval

The participants in this were recruited from Yenepoya Medical College Hospital, Mangalore, with approval from the Yenepoya Ethics Committee-1 (Protocol no. YEC-1/2020/050). The in vivo study procedures were followed as per the approval from Yenepoya University Institutional Animal Ethics Committee (Approval number: YU/IAEC/P06/2024).

Additional information

Supplementary Information The online version contains supplementary material available at https://doi.org/10.1038/s41598-025-94666-y.

Correspondence and requests for materials should be addressed to R.P.S., A.H., T.S.K.P. or F.-T.S.

Reprints and permissions information is available at www.nature.com/reprints.

Publisher's note Springer Nature remains neutral with regard to jurisdictional claims in published maps and institutional affiliations.

Open Access This article is licensed under a Creative Commons Attribution-NonCommercial-NoDerivatives 4.0 International License, which permits any non-commercial use, sharing, distribution and reproduction in any medium or format, as long as you give appropriate credit to the original author(s) and the source, provide a link to the Creative Commons licence, and indicate if you modified the licensed material. You do not have permission under this licence to share adapted material derived from this article or parts of it. The images or other third party material in this article are included in the article's Creative Commons licence, unless indicated otherwise in a credit line to the material. If material is not included in the article's Creative Commons licence and your intended use is not permitted by statutory regulation or exceeds the permitted use, you will need to obtain permission directly from the copyright holder. To view a copy of this licence, visit http://creativecommons.org/licenses/by-nc-nd/4.0/.

© The Author(s) 2025